

Mechanism of Misorientation Development within Coalesced Martensite

Junhak Pak*, H. K. D. H. Bhadeshia*,[‡] and L. Karlsson[†]

*Graduate Institute of Ferrous Technology (GIFT)
Pohang University of Science and Technology (POSTECH)
Pohang 790-784, Republic of Korea, cml.postech.ac.kr

[‡]University of Cambridge
Materials Science and Metallurgy, Cambridge CB2 3QZ, U.K.

[†]ESAB AB, Central Research Laboratories
40277 Goteborg, Sweden

Abstract

Coarse crystals of martensite can form by the coalescence of thin, individual platelets of martensite under appropriate circumstances. Although these coarse grains are essentially single-crystals, there exist significant orientation gradients across their dimensions. It is demonstrated that these gradients arise because of the plasticity induced in the austenite due to the transformation strain associated with martensite growth. The resulting localised change in austenite orientation is then inherited by new martensite growth which consumes the deformed austenite.

1 Introduction

One of the attractive features of bainite or martensite is that thickness of the individual plates can be extremely small, some 20–40 nm in steels which form bainite at temperatures less than 200°C [1–4]. The thickness increases at higher transformation temperatures typical of conventional alloys, to about 0.2 μm in normal bainitic steels [5–7].

A fine structure is conducive to a good combination of strength and toughness, but it has been discovered that there are circumstances where adjacent platelets of bainite which share the same habit plane and variant of the orientation relationship with austenite tend to impinge and coalesce in the absence of intervening phases [7–12]. The subject has been reviewed [13] and a typical micrograph of a coarse coalesced-bainite plate is illustrated in Fig. 1; a three-dimensional characterisation using focused ion beam tomography has been reported [14]. It has been demonstrated that eliminating this coarsening process results in significantly improved toughness [11, 15, 16].

As already stated, large plates, such as the one illustrated in Fig. 1, form as a consequence of the coalescence of finer platelets which are independently nucleated but share the same crystallography with the parent austenite. It has been shown therefore, using electron back scatter diffraction, that large plates which are a consequence of coalescence are essentially single crystals, but nevertheless contain orientation gradients of about $0.3^\circ/\mu\text{m}$ [17]. Considering the common characteristics involved in bainite and martensite growth [18], there is no reason to exclude the coalescence in martensitic structure once the large strain energy is available. The process has previously been described for isothermal martensite in an iron alloy [19]. In this work, therefore, the coalescence in martensitic structure was explored and explained, especially focusing on the origin of the orientation gradients.

2 Experimental Method

The alloy used is a weld metal described elsewhere in detail [20], but the chemical composition is given in Table 1, chosen because of the propensity of this alloy to form coalesced bainite. Following austenitisation at 950°C for 5 min the sample was held at 385°C for 2000s and then cooled continuously to obtain martensite.

Transmission electron microscopy was carried on a sample prepared specifically from a grain of coalesced martensite using the focused ion beam technique, with the ion beam accelerating voltage reduced from 30 kV to 5 kV for the final delicate milling.

3 Dilatometry

The whole dilatometry curve, including isothermal processes are presented in Fig. 2(a). The isothermal transformation was performed in the region indicated by the arrow (Fig. 2(b)). It is evident that the bainite hardly formed and the subsequent quenching induced almost fully martensitic transformation. The martensite-start temperature was measured as $337 \pm 2^\circ\text{C}$ using the offset method [21] as shown in Fig. 3.

4 Microscopy and Diffraction

The martensitic structure produced from the dilatometric experiments consists of fine platelets and abnormally large structures (Fig. 4(a)), where the latter correspond to the typical coalesced structures (Fig. 4(b, c)) [11]. Fig. 5 shows a large plate of coalesced martensite in the region marked ‘A’, surrounded by the ordinary fine plates of martensite in the area designated ‘B’. Referring to the axes on Fig. 5, the plane of observation in the transmission electron microscope was xz to ensure that the features observed correspond only to the coalesced structure. The transmission electron micrograph in Fig. 6 shows surprising detail, with evidence of the original platelets which integrated to form the coalesced plate in Fig. 5. The boundaries between the platelets are visible, indicating

that there may have been small misorientations between the platelets before they coalesced.

The electron diffraction patterns from ferrite-platelets A, B and C, shown in Fig. 7 show that they are similarly oriented. However, the pattern from D could not be unambiguously indexed so the sample was tilted to generate the pattern in Fig. 8; this indicated that the relationship between A and D could be described by a rotation of 9.4° about $\langle \bar{1} 1 0 \rangle_\alpha$ which is crystallographically equivalent to 180° about $[0.650 \ 0.054 \ 0.758]_\alpha$ where this axis is close to a diad, i.e., a small misorientation. In other words, all the platelets A–D which form the coalesced plate have small relative misorientations.

5 Mechanism for Orientation Gradients

The shape deformation during the formation of bainite is an invariant-plane strain with a large shear component, a shear strain of about 0.26 on the habit plane [22]. A deformation like this is difficult to sustain elastically at the high temperatures where bainite forms, because the yield strength of austenite is low at elevated temperatures. Direct observations have shown this accommodation occurs in a manner that compensates for the transformation shear [22]. Transmission microscopy of samples in which some austenite is preserved following the growth of bainite has at the same time shown that the plastic accommodation creates a large dislocation density in the austenite adjacent to the bainite [23]. Two things should be noticed; first, plastic accommodation can also happen even during martensite transformation when the austenite fails to accommodate the deformation fully elastically; second, systematic plasticity of this kind may change the effective crystallographic orientation in the deformed region [24]. In fact, Miyamoto *et al.* [25] revealed that austenite adjacent to a platelet of martensite as well as bainite has curved planes due to this very effect.

Therefore a mechanism was proposed to induce small misorientations between plates which in a perfect crystal of austenite would be in exactly the same crystallographic disposition in space. Edge dislocations present within the material only cause curvature of the lattice if there is an excess of positive or negative dislocations (extra half-planes pointing above or below the slip plane respectively). Fig. 9a illustrates the bending of glide planes caused by the presence of an excess density of edge dislocations with the same sign, the tilt being about an axis on the slip plane normal to the Burgers vector (of magnitude b). Suppose that the excess dislocation density localised into a region with width L (Fig. 9b); assuming a unit depth, the product ρL gives the number of dislocations per unit length and its inverse the spacing between the dislocations in the array which forms the tilt boundary. It follows that for small misorientations, the misorientation θ about the line vector is given by

$$\theta = b\rho L. \quad (1)$$

The Burgers vector for slip in austenite is $\frac{1}{2}a_\gamma \langle 110 \rangle$ so that $b = 2.548 \text{ \AA}$ for a lattice parameter of $a_\gamma = 3.604 \text{ \AA}$. The dimension L representing the deformed austenite adjacent to the bainite plate is taken to be equal to the typical width of the plate, $0.2 \mu\text{m}$. Here ρ is the dislocation density. Dislocations in martensite and bainite formed at high temperatures are inherited from the austenite deformed to be compatible to the transformation strain, so the dislocation density in the product should be the same as that in the parent [26]. The density ρ can therefore be estimate using an

empirical equation available in the literature:

$$\log \left\{ \frac{\rho}{\text{m}^{-2}} \right\} \simeq 9.2848 + \frac{6880}{T} - \frac{1780360}{T^2} \quad \text{for } 570 < T < 920 \text{ K} \quad (2)$$

where T is the absolute temperature at which the microstructure is generated. For martensite formed at 337°C , $\rho = 6.01 \times 10^{15} \text{ m}^{-2}$.

Considering that the growth of martensite is identical to that of bainite crystallographically and that the plastic accommodation is allowed in austenite, the habit plane of martensite is assumed to be that given by Davenport [27] as approximately $(232)_\gamma$ as illustrated in Fig. 9. Austenite slips on the system consisting of close-packed planes and directions $\{111\} <1\bar{1}0>$ so that the slip direction approximately lies within the habit plane. Given that the habit plane is not a close-packed plane of austenite, it requires a combination of slip systems to accommodate the transformation shear (we have neglected the smaller volume change due to transformation). Using well-established Taylor theory for the operation of multiple slip systems to account for an arbitrary plastic deformation [28], it was found that the simultaneous operation of the slip systems $(111)[\bar{1}01]$ and $(1\bar{1}1)[10\bar{1}]$ with the shear strain due to the former being five times that of the latter, can accommodate the shape deformation of martensite. The full description for the calculation is available in [29].

We now proceed to estimate the rotation of the austenite lattice caused by this multiple slip, assuming the model illustrated in Fig. 9. Equation 2 gives the total dislocation density rather than the *excess* density which is not known and will be a fraction ϕ of the total. Three values of the excess quantity were therefore tried, 0.25ρ , 0.5ρ and 0.75ρ , where ρ is the total dislocation density.

The rotation caused by the multiple slip does depend on the order in which the slip systems operate so four combinations of rotations were calculated as listed in Table 2. The results show that the magnitudes of the rotations can be, as expected, small under appropriate *excess* density. It is interesting that the rotation axes listed are all approximately parallel to $[\bar{1}1\bar{1}]_\gamma$, which corresponds to $[101]_\alpha$, given the orientation relationship between martensite and austenite. $[101]_\alpha$ is of course the diad derived previously. Nevertheless, the detailed comparison of the axis-angle pairs with observations is not possible because the specific crystallographic variants of the habit planes and shape deformations of the structure illustrated in Fig. 6 cannot be determined from the thin foil studies. Note also that it is not possible to compare the axis-angle pairs derived using the earlier electron diffraction data because they do not include information about the axis of rotation.

6 Conclusions

It appears that the large plates which form by the coalescence of individual platelets of martensite retain vestiges of their origins, since the boundaries of the original platelets are visible in transmission electron micrographs. This is because the platelets are not precisely identically oriented in space but have small relative rotations. These results are identical to those reported for the coalescence of bainite.

The rotations are explained on the basis that the shape deformation accompanying the formation of a martensite plate causes plastic strain in the adjacent austenite. This in turn changes the

crystallographic orientation of the adjacent austenite, so that a new plate of martensite which grows from this deformed austenite will be slightly rotated relative to the original platelet.

An estimate of the degree of resulting rotation gives reasonable numbers although it has not been possible to attain a quantitative comparison with experimental observations because the latter are incomplete due to the fine scale of the structure and because of the absence of austenite. A complete closure with theory would require the three-dimensional crystallography (habit plane, shape deformation and orientation relationship) to be characterised.

Acknowledgments

We are grateful to the technical staff at the NCNT-POSTECH for help with the TEM and FIB work, to Jee Hyun Kang and Joo Hyun Ryu for discussions. The work was funded by the Steel Innovation Program of POSCO and the World Class University programme R32-2008-000-10147-0 of the National Research Foundation of Korea.

References

- [1] C. Garcia-Mateo, F. G. Caballero, and H. K. D. H. Bhadeshia. Development of hard bainite. *ISIJ International*, 43:1238–1243, 2003.
- [2] P. M. Brown and D. P. Baxter. Hyper-strength bainitic steels. In *Materials Science and Technology 2004*, pages 433–438, Warrendale, Pennsylvania, USA, 2004. TMS.
- [3] M. Kundu, S. Ganguly, S. Datta, and P. P. Chattopadhyay. Simulating time temperature transformation diagrams of steels using artificial neural networks. *Materials and Manufacturing Processes*, 24:169–173, 2009.
- [4] H. K. D. H. Bhadeshia. Nanostructured bainite. *Proceedings of the Royal Society of London A*, 466:3–18, 2010.
- [5] F. B. Pickering. Mechanism of bainite formation in low-alloy steels containing up to 0.4% carbon. In *4th International Conference on Electron Microscopy*, pages 626–637. Springer Verlag, Berlin, 1958.
- [6] J. P. Naylor and P. R. Krahe. The effect of bainite packet size on toughness. *Metallurgical Transactions*, 5:1699–1701, 1974.
- [7] L. C. Chang and H. K. D. H. Bhadeshia. Microstructure of lower bainite formed at large undercoolings below the bainite start temperature. *Materials Science and Technology*, 12:233–236, 1996.
- [8] R. Padmanabhan and W. E. Wood. Occurrence of blocky martensite in 300M steel. *Materials Science and Engineering*, 66:1–11, 1984.

- [9] E. Keehan, H.-O. Andrén, L. Karlsson, M. Murugananth, and H. K. D. H. Bhadeshia. Microstructural and mechanical effects of nickel and manganese on high strength steel weld metals. In S. A. David and T. DebRoy, editors, *Trends in Welding Research*, pages 695–700. ASM, USA, 2002.
- [10] E. Keehan. Microstructure and properties of novel high strength steel weld metals. *Welding Research Abroad*, 52:1–13, 2006.
- [11] E. Keehan, L. Karlsson, and H.-O. Andrén. Influence of C, Mn and Ni on strong steel weld metals: Part 1, effect of nickel. *Science and Technology of Welding and Joining*, 11:1–8, 2006.
- [12] L.-E. Svensson. Microstructure and properties of high strength weld metals. *Materials Science Forum*, 539–543:3937–3942, 2007.
- [13] H. K. D. H. Bhadeshia, E. Keehan, L. Karlsson, and H. O. Andrén. Coalesced bainite. *Transactions of the Indian Institute of Metals*, 59:689–694, 2006.
- [14] E. Keehan, L. Karlsson, H. K. D. H. Bhadeshia, and M. Thuvander. Three-dimensional analysis of coalesced bainite using focused ion beam tomography. *Materials Characterization*, 59:877–882, 2008.
- [15] F. G. Caballero, J. Chao, J. Cornide, C. Garcia-Mateo, M. J. Santofimia, and C. Capdevila. Toughness deterioration in advanced high strength bainitic steels. *Materials Science & Engineering A*, 525:87–95, 2009.
- [16] F. G. Caballero, J. Chao, J. Cornide, C. Garcia-Mateo, M. J. Santofimia, and C. Capdevila. Toughness of advanced high strength bainitic steels. *Materials Science Forum*, 638–642:118–123, 2010.
- [17] E. Keehan, L. Karlsson, H. K. D. H. Bhadeshia, and M. Thuvander. Electron backscattering diffraction study of coalesced bainite in high strength steel weld metals. *Materials Science and Technology*, 24:1183–1188, 2008.
- [18] H. K. D. H. Bhadeshia. Design of ferritic creep-resistant steels. *ISIJ International*, 41:621–640, 2001.
- [19] D. Yang and M. Zhu. Growth of isothermal martensite in an Fe–Ni–Mn alloy. *Acta Metallurgica Sinica*, 24:236–241, 1988.
- [20] J. H. Pak, H. K. D. H. Bhadeshia, L. Karlsson, and E. Keehan. Coalesced bainite by isothermal transformation of reheated weld metal. *Science and Technology of Welding and Joining*, 13:593–597, 2008.
- [21] H.-S. Yang and H. K. D. H. Bhadeshia. Uncertainties in the dilatometric determination of the martensite-start temperature. *Materials Science and Technology*, 23:556–560, 2007.
- [22] E. Swallow and H. K. D. H. Bhadeshia. High resolution observations of displacements caused by bainitic transformation. *Materials Science and Technology*, 12:121–125, 1996.
- [23] H. K. D. H. Bhadeshia and D. V. Edmonds. The bainite transformation in a silicon steel. *Metallurgical Transactions A*, 10A:895–907, 1979.
- [24] J. W. Christian. Simple geometry and crystallography applied to ferrous bainites. *Metallurgical transactions A*, 21:799–803, 1990.

- [25] G. Miyamoto, A. Shibata, T. Maki, and T. Furuhashi. Precise measurement of strain accommodation in austenite matrix surrounding martensite in ferrous alloys by electron backscatter diffraction analysis. *Acta Materialia*, 57:1120–1131, 2009.
- [26] J. W. Christian. Thermodynamics and kinetics of martensite. In G. B. Olson and M. Cohen, editors, *International Conference on Martensitic Transformations ICOMAT '79*, pages 220–234, 1979.
- [27] A. T. Davenport. The crystallography of upper bainite. Technical Report Project 12051, Republic Steel Research Center, Ohio, USA, February 1974.
- [28] D. N. Lee. *Texture and related phenomena*. Korean Institute of Metals and Materials, Seoul, Republic of Korea, 2006.
- [29] J. H. Pak, D. W. Suh, and H. K. D. H. Bhadeshia. Bainite: Fragmentation of crystallographically homogeneous domains. *International Journal of Materials Research*, 103:1–7, 2012.

Table 1: Chemical composition of the weld deposit studied, wt%

C	Si	Mn	P	S	Cr	Ni	Mo	W
0.03	0.23	2.05	0.01	0.008	0.43	7.1	0.63	0.004
Co	V	Nb	Cu	Al	Ti	B	O	N
0.008	0.021	0.004	0.02	0.001	0.011	0.0012	0.031	0.011

Table 2: Rotation axis and angle derived from the operation slip systems $a \equiv (111)[\bar{1}01]$ and $b \equiv (1\bar{1}1)[10\bar{1}]$. R represents the rotation operation with the sequence of operation from right to left. All of the stated indices are with respect to austenite.

ϕ	$R_b R_a$	$\frac{1}{2}R_b \frac{1}{2}R_a \frac{1}{2}R_b \frac{1}{2}R_a$	$\frac{1}{2}R_a \frac{1}{2}R_b \frac{1}{2}R_a \frac{1}{2}R_b$	$R_a R_b$
0.25	3.48° [0.519 0.686 0.510]	3.48° [0.517 0.686 0.512]	3.48° [0.512 0.686 0.517]	3.48° [0.510 0.686 0.519]
0.50	6.96° [0.523 0.686 0.505]	6.96° [0.519 0.686 0.510]	6.96° [0.510 0.686 0.519]	6.96° [0.505 0.686 0.523]
0.75	10.44° [0.528 0.686 0.501]	10.44° [0.521 0.686 0.508]	10.44° [0.508 0.686 0.521]	10.44° [0.501 0.686 0.528]

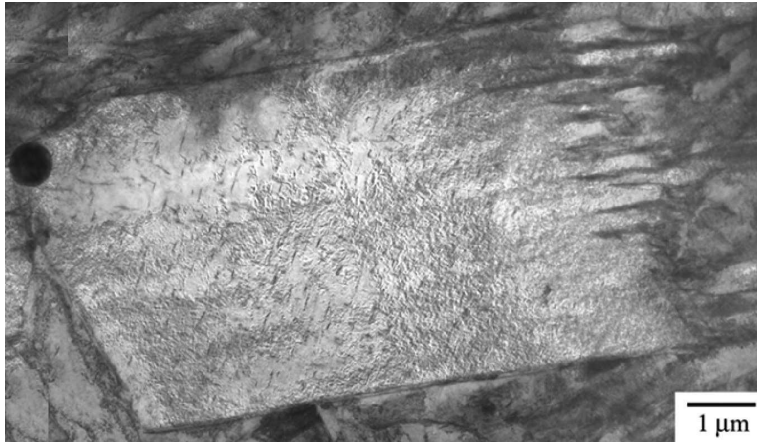
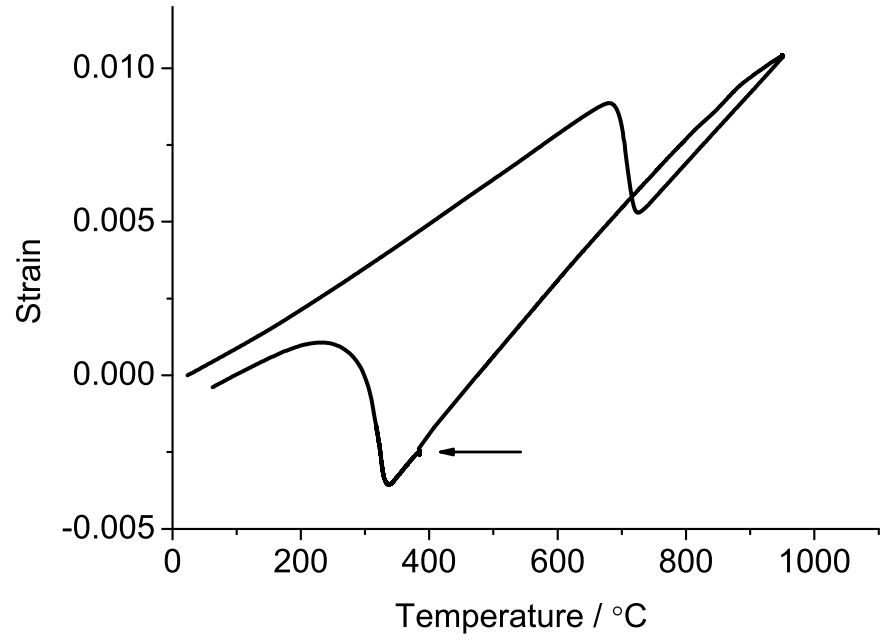
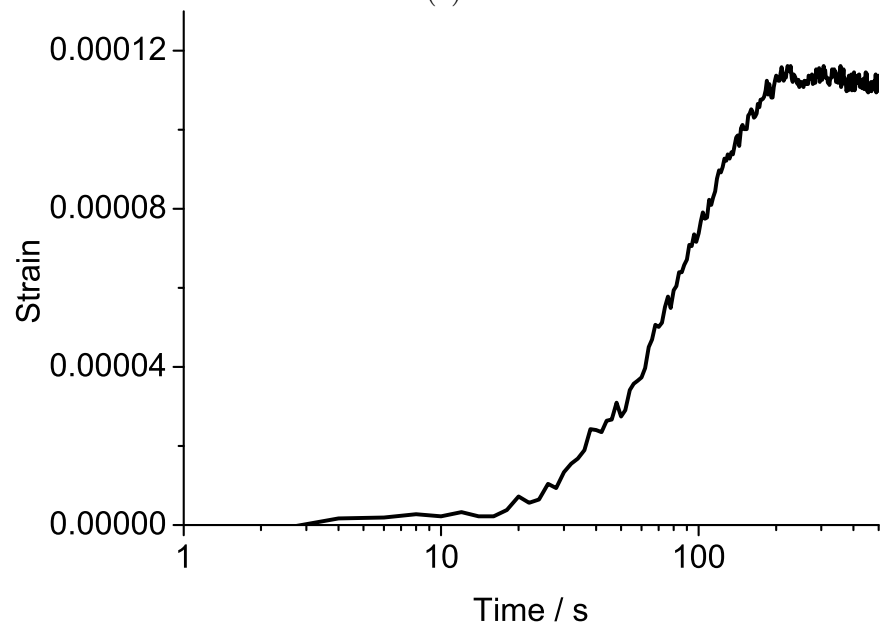


Figure 1: Coarse plate of coalesced bainite, many micrometres in thickness, forming by the coalescence of finer platelets which are visible towards the right hand side [11].



(a)



(b)

Figure 2: Dilatometry curve for (a) whole temperature range and (b) isothermal transformation at 385 °C

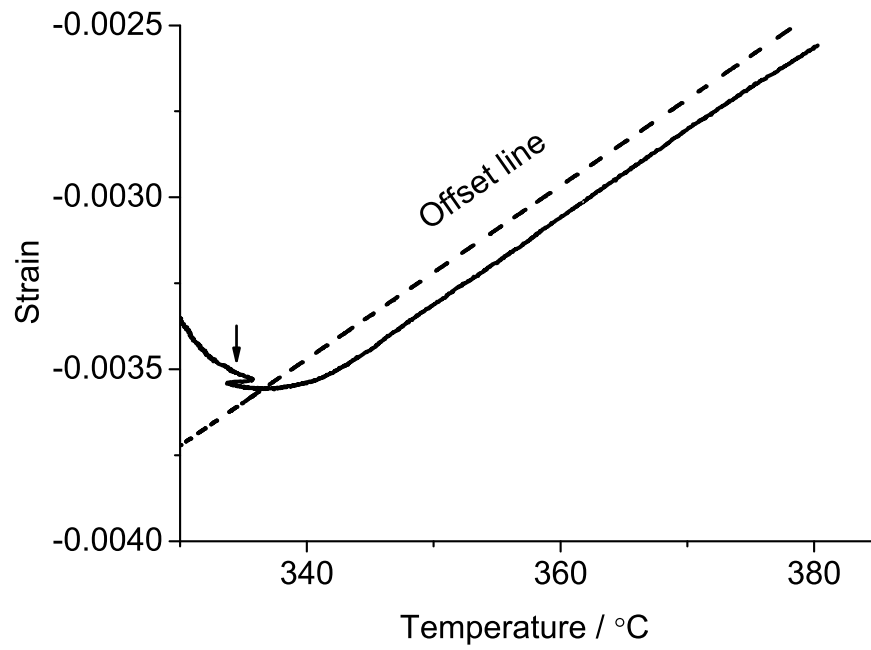
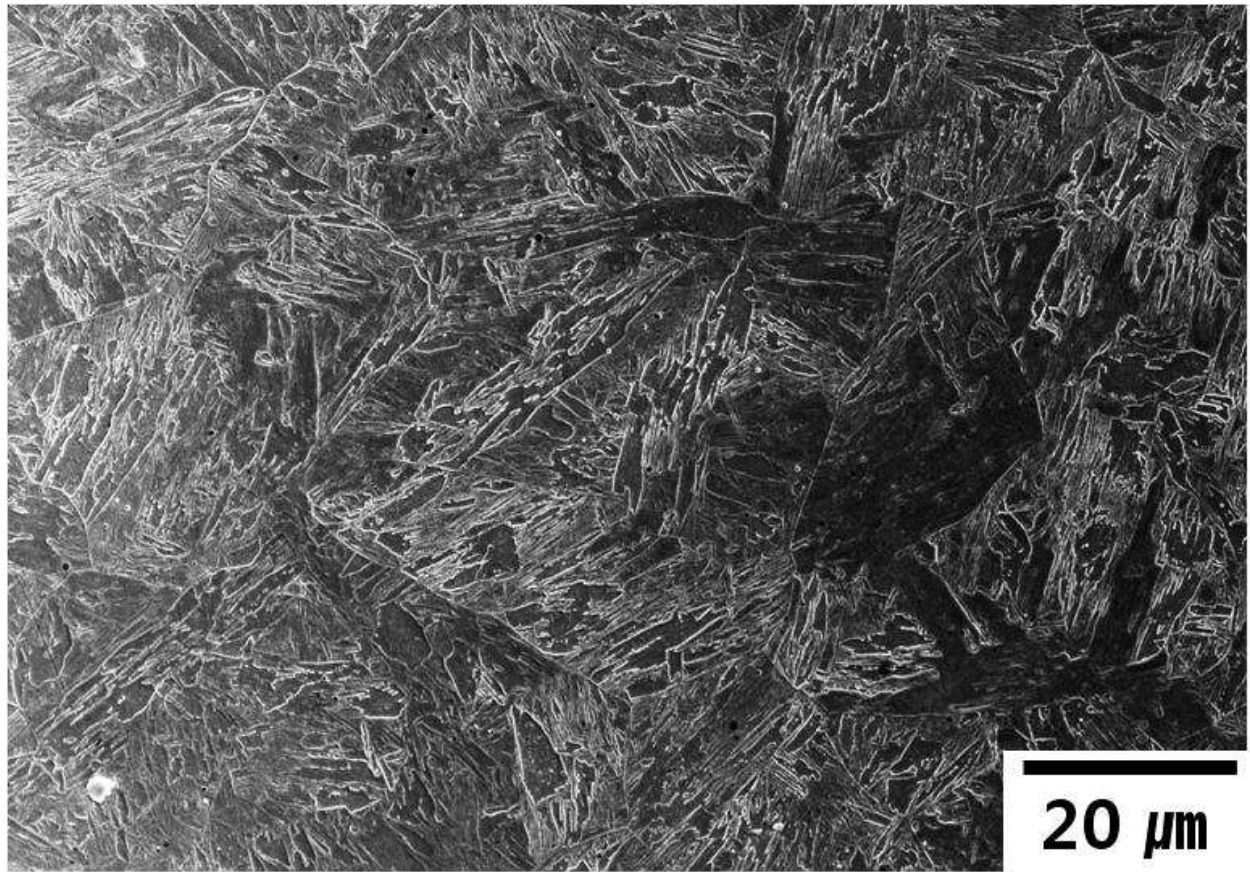
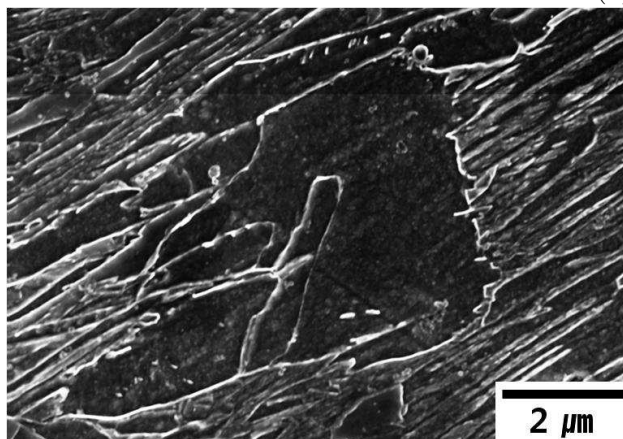


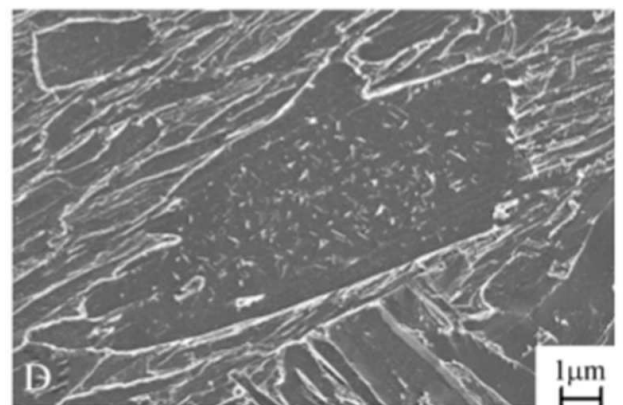
Figure 3: Illustration to find the start temperature of martensite transformation following the isothermal process. Dotted line corresponds to the offset line and the irregular curve indicated by the arrow is due to the unstable cooling in the machine.



(a)



(b)



(c)

Figure 4: Observation using scanning electron microscopy; (a) the overall microstructure; (b) the observed coalesced structure; (c) the reported coalesced bainite [11]

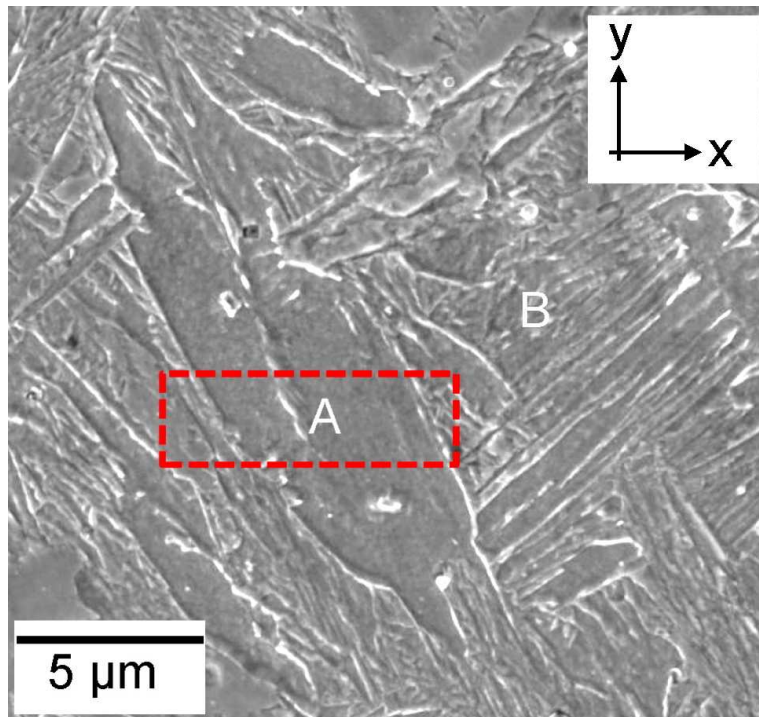


Figure 5: Coalesced (A) and fine martensite (B) in focused ion beam micrograph. The marked rectangle indicates the area from which the transmission electron microscopy sample was extracted.

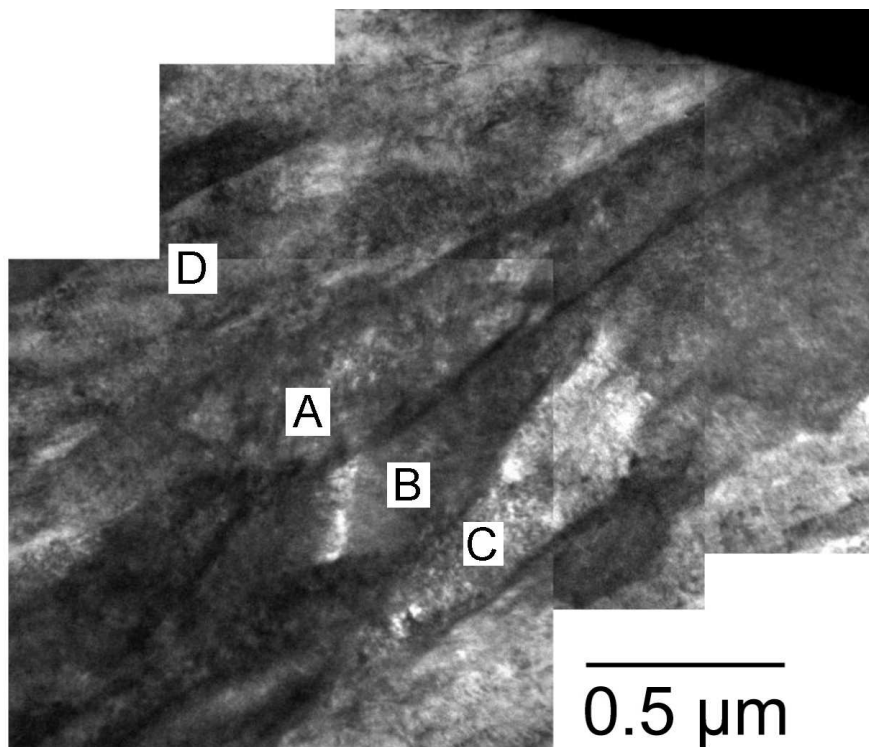


Figure 6: Transmission electron micrograph montage representing coalesced martensite illustrated in Fig. 5.

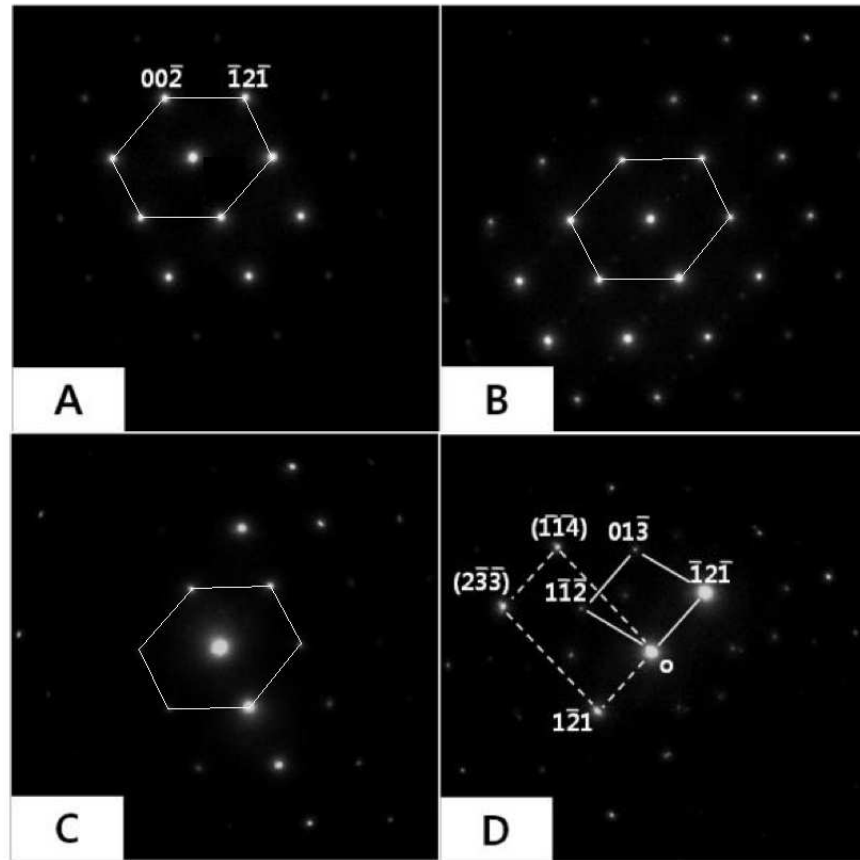


Figure 7: Diffraction patterns from each of the platelets marked in Fig. 6. A, B and C are similarly oriented but the pattern from D is ambiguous.

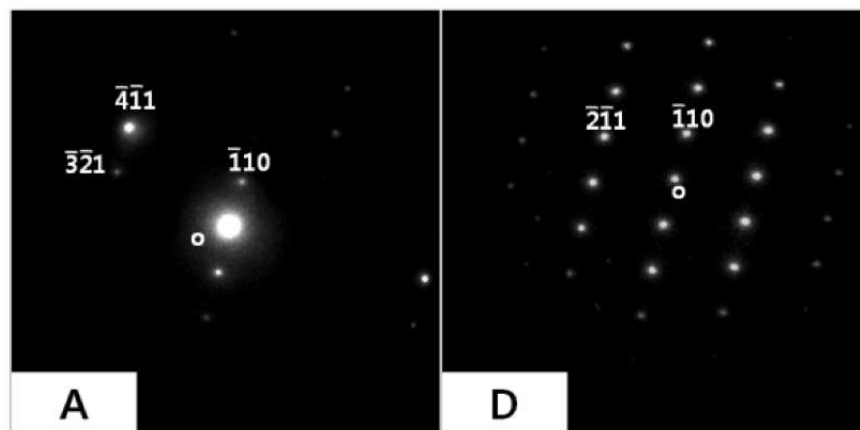


Figure 8: Diffraction patterns from platelets A and D marked in Fig. 6 after tilting relative to the patterns shown in Fig. 7.

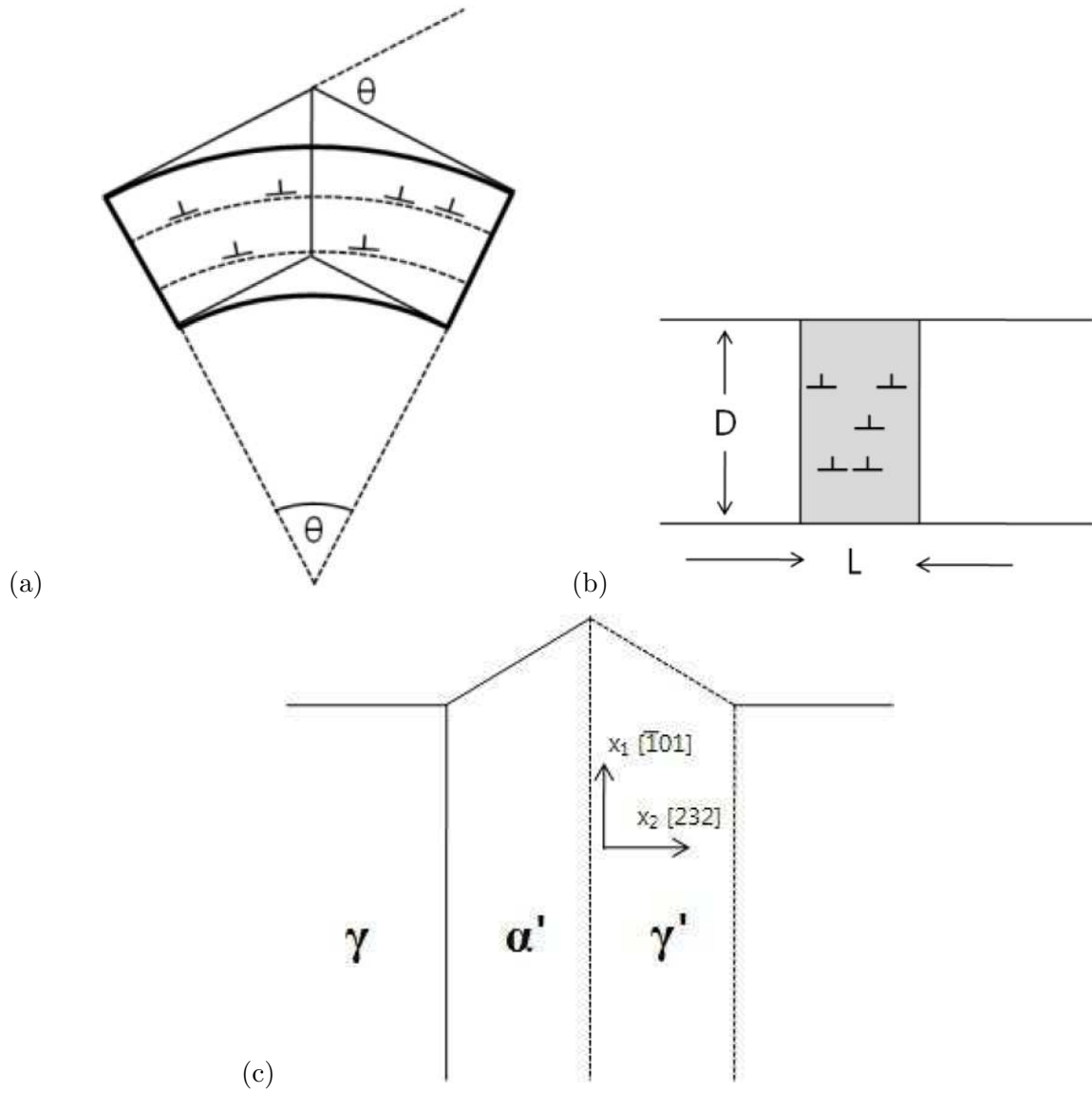


Figure 9: (a) Dislocations causing the development of misorientation in a single crystal. (b) Excess dislocations in the grey area, assumed to align into a column to cause a constant misorientation between the adjacent white areas. (c) Plastic accommodation in the austenite. The region enclosed by the dashed lines represents deformed austenite, the upheaval being caused by the shape deformation accompanying the growth of martensite.